Contents lists available at ScienceDirect

Nuclear Inst. and Methods in Physics Research, A

Preliminary RF design of an X-band linac for the EuPRAXIA@SPARC_LAB project

M. Diomede [a,b,*], D. Alesini [b], M. Bellaveglia [b], B. Buonomo [b], F. Cardelli [b], N. Catalan Lasheras [c], E. Chiadroni [b], G. Di Pirro [b], M. Ferrario [b], A. Gallo [b], A. Ghigo [b], A. Giribono [b], A. Grudiev [c], L. Piersanti [b], B. Spataro [b], C. Vaccarezza [b], W. Wuensch [c]

[a] Sapienza University, Piazzale Aldo Moro 5, Roma, Italy
[b] INFN-LNF, Via E. Fermi 40, Frascati, Italy
[c] CERN, CH-1211 Geneva-23, Switzerland

ABSTRACT

In the framework of the upgrade of the SPARC_LAB facility at INFN-LNF (Frascati, Italy), named EuPRAXIA@SPARC_LAB, a high gradient linac is foreseen. One of the most suitable options is to realize it in X-band. A preliminary design study of both accelerating structures and power distribution system has been performed. It is based on 0.5 m long traveling wave (TW) accelerating structures operating in the $2\pi/3$ mode and fed by klystrons and pulse compressor systems. The main parameters of the structures and linac are presented with the basic RF linac layout.

1. Introduction

In the framework of research and development of novel acceleration schemes and technology, the upgrade of the SPARC_LAB test facility [1] at INFN-LNF (Frascati, Italy) is foreseen, based on a high gradient linac. High brightness electron bunches are fundamental for the successful development of plasma-based accelerators, for instance, whereas external injection schemes are considered, i.e. particle beam driven and laser driven plasma wakefield accelerators (PWFA and LWFA, respectively). Indeed, the ultimate beam brightness and its stability and reproducibility are strongly influenced by the RF-generated electron beam.

In this scenario the SPARC_LAB upgrade, named as EuPRAXIA@SPARC_LAB [2], might be one of the possible candidates to host EuPRAXIA (European Plasma Research Accelerator with eXcellence In Applications) [3]. EuPRAXIA is a design study in the framework of Horizon 2020 (INFRADEV-1-2014), funded to bring together for the first time novel acceleration schemes, based for instance on plasmas, modern lasers, the latest correction/feedback technologies and large-scale user areas. Such a research infrastructure would achieve the required quantum leap in accelerator technology towards more compact and more cost-effective accelerators, opening new horizons for applications and research.

The preliminary EuPRAXIA@SPARC_LAB linac layout is based on an S-band Gun, three S-band TW structures and an X-band booster with a bunch compressor [2]. The booster design has been driven by the need of a high accelerating gradient required to achieve a high facility compactness, which is one of the main goals of the EuPRAXIA project. The baseline technology chosen for the EuPRAXIA@SPARC_LAB booster is X-band. The total space allocated for the linac accelerating sections is ≈25 m, corresponding to an active length of ≈16 m taking into account the space required to accommodate beam diagnostics, magnetic elements, vacuum equipment and flanges. Two average accelerating gradient options are foreseen for the X-band linac: high gradient (HG) of 57 MV/m and very high gradient (VHG) of 80 MV/m, corresponding to double the power of the HG case. The RF linac layout is based on klystrons with SLEDs [4] that feed several TW accelerating structures. The operating mode is the $2\pi/3$ mode at 11.9942 GHz. The preliminary RF system parameters are summarized in Table 1 [5].

In this paper we illustrate the preliminary RF design of the X-band booster. The single cell parameters have been calculated by electromagnetic (e.m.) simulations. On the basis of these results, the accelerating structure length and geometry have been optimized by numerical studies. Finally, the basic RF power distribution layout has been designed.

---

* Corresponding author.
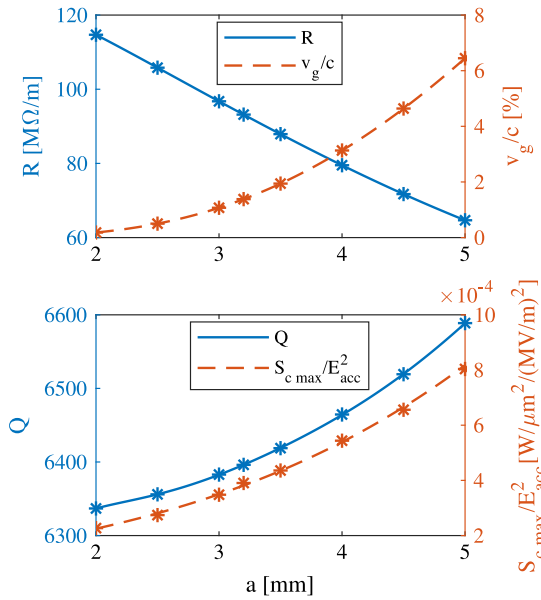*E-mail address:* marco.diomede@uniroma1.it (M. Diomede).

Fig. 1. Single cell parameters as a function of the iris radius.

Table 1
RF system parameters.

Frequency	11.9942 GHz
Peak RF power	50 MW
RF pulse length t_k	1.5 μs
Unloaded Q-factor Q_0 of SLED	180 000

Table 2
Single cell parameters for an iris radius of 3.2 mm.

Iris radius a [mm]	3.2
Iris thickness t [mm]	2.5
Cell radius b [mm]	10.139
Cell length d [mm]	8.332
R [MΩ/m]	93
v_g/c [%]	1.382
Q	6396
$S_{c\,max}/E_{acc}^2$ [A/V]	$3.9 \cdot 10^{-4}$

2. Single cell study

The main single cell parameters (shunt impedance per unit length R, normalized group velocity v_g/c, Q-factor Q, peak value of modified Poynting vector [6,7] normalized to the average accelerating field $S_{c\,max}/E_{acc}^2$) as a function of the iris radius a have been calculated with ANSYS Electronics Desktop [8]. The results are reported in Fig. 1.

According to beam dynamics calculations and single bunch beam break up limits, an average iris radius $\langle a \rangle = 3.2$ mm has been taken into account (the corresponding parameters are given in Table 2) [9].

3. Analytical optimization of structure effective shunt impedance

The accelerating gradient distribution along the structure after one filling time t_f is given by the formula [10]:

$$G(z, t_f) = G_0[t_f - \tau(z)]g(z), \tag{3.1}$$

where z is the longitudinal position, $\tau(z) = \int_0^z \frac{dz'}{v_g(z')}$ is the signal time delay and $g(z)$ is defined as:

$$g(z) = \sqrt{\frac{v_g(0)}{v_g(z)}} \sqrt{\frac{R(z)Q(0)}{R(0)Q(z)}} e^{-\frac{1}{2} \int_0^z \frac{\omega}{v_g(z')Q(z')} dz'}. \tag{3.2}$$
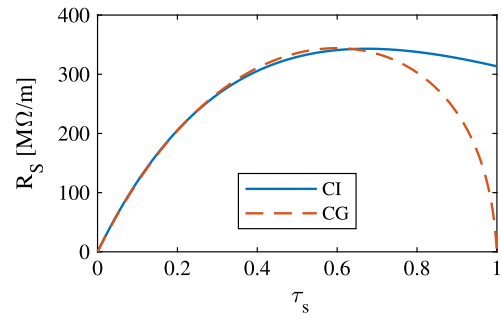

Fig. 2. Effective shunt impedance per unit length for the CI and CG structure.

G_0 is the gradient at the beginning of the structure given by:

$$G_0(t) = \sqrt{\frac{\omega R(0)P_0(t)}{v_g(0)Q(0)}}. \tag{3.3}$$

$P_0(t)$ is the input RF power and, due to the SLED, is given by:

$$P_0(t) = P_k \cdot k_{SLED}^2(t), \tag{3.4}$$

where P_k is the power from the klystron and $k_{SLED}(t)$ is the SLED electric field gain factor [4].

Integrating Eq. (3.1) along the structure length L_s, we obtain the accelerating voltage V_a.

The efficiency of the structure is given by the effective shunt impedance per unit length R_s defined as [11]:

$$R_s = \frac{V_a^2}{P_k L_s} = \frac{V_a \langle G \rangle}{P_k} = \frac{\langle G \rangle^2 L_s}{P_k}, \tag{3.5}$$

where $\langle G \rangle = V_a / L_s$ is the average accelerating gradient.

For a constant impedance (CI) structure R_s, as a function of the section attenuation $\tau_s \ (= \frac{\omega}{2 v_g Q} L_s)$, is given by [12]:

$$R_s = 2\tau_s R \left\{ \frac{1 - \frac{2Q_l}{Q_e}}{\tau_s} (1 - e^{-\tau_s}) \right.$$
$$\left. + \frac{\frac{2Q_l}{Q_e} \left[2 - e^{-\left(\frac{\omega t_k}{2Q_l} - \tau_s \frac{Q}{Q_l} \right)} \right]}{\tau_s \left(1 - \frac{Q_l}{Q_e} \right)} \left(e^{-\tau_s \frac{Q_l}{Q_e}} - e^{-\tau_s} \right) \right\}^2, \tag{3.6}$$

where $Q_l = \frac{Q_0 Q_e}{Q_0 + Q_e}$ is the loaded Q-factor of SLED (being Q_e the external quality factor). For a constant gradient (CG) structure R_s is given by [4]:

$$R_s = R \frac{2\tau_s}{1 + \tau_s} \left\{ 1 - \frac{2Q_l}{Q_e} + \frac{2Q_l}{Q_e} \left[2 - e^{-\frac{\omega t_k}{2Q_l}} \left(\frac{1 + \tau_s}{1 - \tau_s} \right)^{\frac{Q}{2Q_l}} \right] \right.$$
$$\left. \cdot \frac{1 - \tau_s}{2\tau_s} \frac{1}{1 - Q/2Q_l} \left[\left(\frac{1 + \tau_s}{1 - \tau_s} \right)^{1 - \frac{Q}{2Q_l}} - 1 \right] \right\}^2. \tag{3.7}$$

Fig. 2 shows R_s as a function of τ_s for both structures, with the parameters of Tables 1 and 2. In both cases the value of the external Q-factor Q_e of the SLED has been chosen in order to maximize R_s.

The accelerating gradient for a CI structure is given by [12]:

$$G(z, t_f) = \sqrt{\frac{\omega}{v_g} \frac{R}{Q} P_k} e^{-\tau_s \frac{z}{L_s}}$$
$$\cdot \left\{ 1 + \frac{2Q_l}{Q_e} \left[e^{-\frac{\omega(L_s - z)}{2 v_g Q_l}} \left(2 - e^{-\frac{\omega(t_k - t_f)}{2Q_l}} \right) - 1 \right] \right\}, \tag{3.8}$$
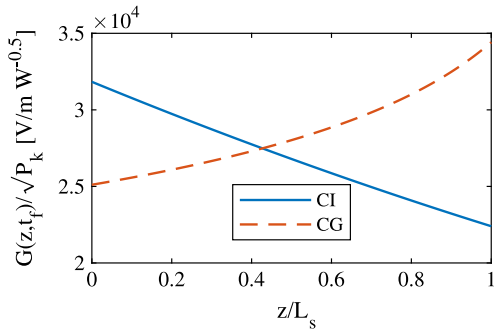
Fig. 3. Normalized gradient distribution along the structure for the CI and CG structure.
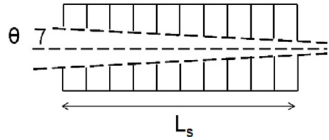

Fig. 4. Sketch of the linear iris tapering.

Table 3
CI and CG structure parameters (analytical study).

Parameter	CI	CG
R_s [MΩ/m]	343	344
Optimal structure length L_s [m]	0.474	0.432
Filling time t_f [ns]	114	118
External Q-factor Q_e of SLED	20 030	21 170

while for a CG structure is given by [4]:

$$G(z, t_f) = \sqrt{\frac{2\tau_s}{1+\tau_s}\frac{R}{L_s}P_k} \left\{ 1 + \frac{2Q_l}{Q_e} \right.$$

$$\left. \cdot \left[\left(\frac{1 + \tau_s\left(1 - \frac{2z}{L_s}\right)}{1 - \tau_s} \right)^{-\frac{Q}{2Q_l}} \left(2 - e^{-\frac{\omega(t_k - t_f)}{2Q_l}} \right) - 1 \right] \right\}. \quad (3.9)$$

The previous formulas (3.6), (3.7) allow calculating the optimum τ_s ($=\tau_{s0}$) that maximize R_s. This fixes also the filling time of the structure, i.e. the compressed pulse length and allows to calculate the corresponding gradient profiles given in Fig. 3.

The final optimum structures parameters are summarized in Table 3.

4. Numerical optimization

In the analytical study, the CG solution is approximated because of the assumption of constant R/Q [13] along the structure. On the other hand in the CI case it is quite easy to verify that, in the VHG case, one exceeds the maximum value of $S_{c\,max}$ that allows to have a Breakdown rate (BDR) lower than 10^{-6} bpp/m [6,7]. For these reasons we also performed a numerical study.

To this purpose we have considered a linear tapering of the irises as sketched in Fig. 4, defined by the modulation angle θ. We have then calculated (by Eq. (3.1)) the gradient profile along the structure for different θ and L_s. In the calculation we have used the polynomial fits of the single cell parameters illustrated in Section 2. From the gradient profiles we have finally calculated the effective shunt impedance per unit length and the peak value of the modified Poynting vector.
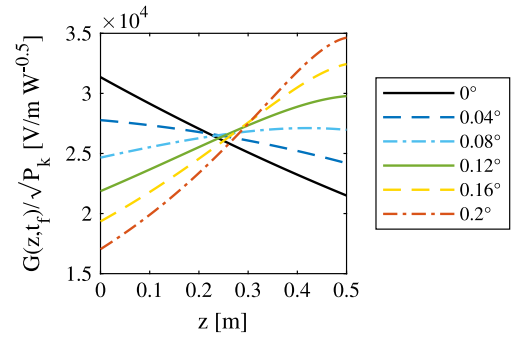

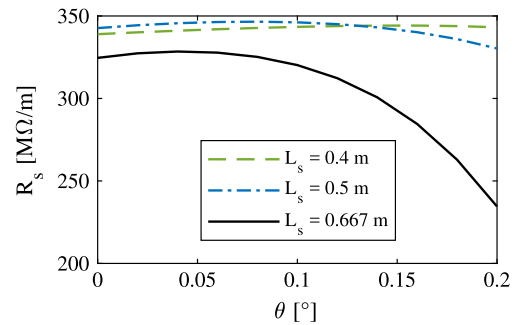**Fig. 5.** Normalized gradient after one filling time as function of the modulation angle (0.5 m case).

Fig. 6. Effective shunt impedance per unit length as a function of the modulation angle for three structure lengths.
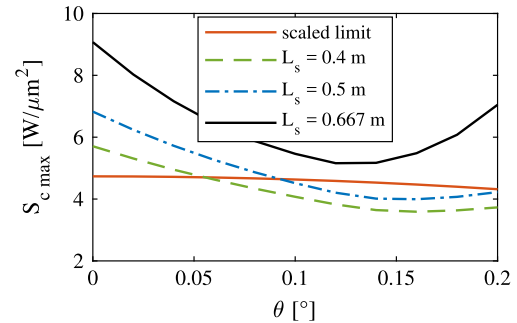

Fig. 7. Peak value of modified Poynting vector as a function of the modulation angle for three structure lengths (VHG case).

Fig. 5 shows, as an example, the normalized gradient profile as a function of θ for L_s equal to 0.5 m. R_s and $S_{c\,max}$ (VHG case), as a function of θ and for different L_s, are given in Figs. 6 and 7. In Fig. 7 we have also reported the maximum value of $S_{c\,max}$ that, according to the scaling law given in [6], allows having a BDR lower than 10^{-6} bpp/m. From the plot it is quite easy to note that the 0.4 m and 0.5 m long structures have the same efficiency while the 0.667 m case is worse. Concerning $S_{c\,max}$, the 0.4 m solution is better but requires, on the other hand, a larger number of structures per unit length. In conclusion the 0.5 m case with $\theta = 0.1°$ has been chosen as the design baseline for the X-band linac.

5. Linac basic layout

According to the results of numerical study, the TW X-band accelerating sections optimized for the EuPRAXIA@SPARC_LAB application are 0.5 m long and show an effective shunt impedance per unit length of 346 MΩ/m. Commercially available X-band klystrons [5] provide up to
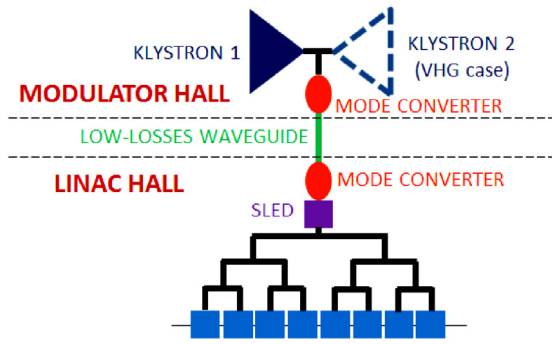
Fig. 8. RF power distribution layout of a single module for the HG and VHG cases.

Table 4
X-band linac parameters.

	HG	VHG
Frequency of operation [GHz]	11.9942	
RF pulse length t_f [ns]	129	
Unloaded Q-factor Q_0 of SLED	180 000	
External Q-factor Q_e of SLED	21 800	
a first-last cell [mm]	3.636 − 2.764	
Structure length L_s [m]	0.5	
Active length L_t [m]	16	
No. of structures N_s	32	
v_g/c first-last cell [%]	2.23 − 0.77	
R_s [MΩ/m]	346	
Average gradient $\langle G \rangle$ [MV/m]	57	80
Energy gain W_{gain} [MeV]	912	1280
Total Required RF power P_{RF} [W]	150	296
No. of klystrons N_k	4	8

50 MW peak power with 1.5 µs long RF pulses. We have estimated the RF losses in the waveguide distribution system of ≈−7 dB and, as a consequence, ≈40 MW available input power. The basic RF module of the EuPRAXIA@SPARC_LAB X-band linac can be conveniently composed by a group of 8 TW sections assembled on a single girder and powered by one (for HG) or two (for VHG) klystrons by means of one pulse compressor system and a waveguide network splitting and transporting the RF power to the input couplers of the sections. The sketch of the

basic module is given in Fig. 8 while the final main linac parameters are shown in Table 4.

6. Conclusions

In the paper we have illustrated the preliminary RF design of the EuPRAXIA@SPARC_LAB X-band linac. It has been done performing e.m. simulations of the single cell, and analytical and numerical optimization of the structure efficiency taking into account the available space, local field quantity (modified Poynting vector) minimization and available commercial klystrons. The final linac layout and main parameters have been finally shown.

Acknowledgment

References

[1] M. Ferrario, et al., SPARC_LAB present and future, Nucl. Instrum. Methods Phys. Res. B 309 (2013) 183–188.
[2] M. Ferrario, et al., EuPRAXIA@SPARC_LAB: design study towards a compact FEL facility at LNF, these proceedings, 2017.
[3] P.A. Walker, et al., HORIZON 2020 EuPRAXIA design study, in: Proc. of IPAC2017, TUOBB3, Copenhagen, Denmark, 2017.
[4] Z. Farkas, H. Hogg, G. Loew, P.B Wilson, SLED: A method of doubling SLAC's energy, in: Proc. of 9th Int. Conf. on High Energy Accelerators, SLAC, 1974, p. 576.
[5] CPI website, http://www.cpii.com/.
[6] A. Grudiev, S. Calatroni, W. Wuensch, New local field quantity describing the high gradient limit of accelerating structures, Phys. Rev. Spec. Top. Accel. Beams 12 (2009) 102001.
[7] K. Sjobak, E. Adli, A. Grudiev, New criterion for shape optimization of normal-conducting accelerator cells for high-gradient applications, in: Proc. of LINAC2014, Geneva, Switzerland, 2014.
[8] ANSYS Electronics Desktop website, http://www.ansys.com/products/electronics/ansys-electronics-desktop.
[9] C. Vaccarezza, et al., EuPRAXIA@SPARC_LAB: Beam Dynamics studies for the X-band Linac, these proceedings, 2017.
[10] A. Lunin, V. Yakovlev, A. Grudiev, Analytical solutions for transient and steady state beam loading in arbitrary traveling wave accelerating structures, Phys. Rev. ST Accel. Beams 14 (2011) 052001.
[11] R.B. Neal, Design of linear electron accelerators with beam loading, J. Appl. Phys. 29 (7) (1958) 1019–1024.
[12] J. Le Duff, High-field electron linacs, in: CERN Yellow Report CERN-95-06, 1995.
[13] P.M. Lapostolle, A.L. Septier, Linear Accelerators, North-Holland, Amsterdam, 1970.